coholate is not sufficiently reactive to substitute for the chlorine in PCl_2 centers of other molecules. Mild acid hydrolysis finally yields products **2**.

Acknowledgment. This work was supported in part (J.C.v.d.G.) by NATO Grant 0043/86. We are indebted to Shin Nisso Kako Co. Ltd., Tokyo, for their generous gift of $(NPCl_2)_3$.

Supplementary Material Available: Table SI, compiling the eluants used in flash chromatographic separations, Table SII, giving microanalytical data, Table SIII, giving IR spectroscopic data, and Table SIV, compiling ^1H NMR and proton-decoupled ^{13}C NMR data (9 pages). Ordering information is given on any current masthead page.

Contribution from the Departments of Chemistry, Colorado State University, Fort Collins, Colorado 80523, and The University of North Carolina, Chapel Hill, North Carolina 27599, Faculty of Integrated Arts & Sciences, Hiroshima University, 1-1-89 Higashisenda, Naka-ku, Hiroshima 730, Japan, and Department of Physics, University of Vermont, Burlington, Vermont 05405

Cytochrome *c* Oxidase Models: Iron(III) Porphyrin–Copper(II) Complexes with Sulfur Bridges

Barbara R. Serr,[1a] Christine E. L. Headford,[1b] Oren P. Anderson,*[,1a] C. Michael Elliot,*[,1a] Cynthia K. Schauer,[1c] Kozo Akabori,[1d] Kevork Spartalian,[1e] William E. Hatfield,[1c] and Brian R. Rohrs[1c]

Received May 31, 1989

Three compounds involving sulfur-bridged Fe(porphyrin)–Cu linkages have been synthesized as models for the active site of cytochrome *c* oxidase: (TBA)$_2$[[Fe(*p*-Cl_4TPP)]$_2$[Cu(MNT)$_2$]$_2$]·C_6H_6 (**1**), (TBA)$_2$[[Fe(*p*-Cl_4TPP)]$_2$[Cu(MNT)$_2$]$_2$]·$2C_6H_6$ (**2**), and (TBA)$_2$[[Fe(*p*-Cl_4TPP)]$_2$[Cu(MNT)$_2$]$_2$]·$3C_6H_6$ (**3**) (TBA$^+$ = tetra-*n*-butylammonium, *p*-Cl_4TPP^{2-} = 5,10,15,20-tetrakis(*p*-chlorophenyl)porphyrinate, MNT^{2-} = *cis*-1,2-dicyanoethylenedithiolate). The structures of **1** (monoclinic, a = 17.222 (4) Å, b = 26.818 (5) Å, c = 27.497 (8) Å, β = 103.84 (2)°, Z = 4, space group $C2/c$, T = 20 °C), of **2** (monoclinic, a = 17.489 (5) Å, b = 26.515 (7) Å, c = 27.006 (11) Å, β = 101.39 (3)°, Z = 4, space group $C2/c$, T = −130 °C), and of **3** (triclinic, a = 13.378 (3) Å, b = 17.356 (2) Å, c = 28.918 (7) Å, α = 104.05 (2)°, β = 99.62 (2)°, γ = 98.38 (2)°, Z = 2, space group $P\bar{1}$, T = −130 °C) have been determined by single-crystal X-ray diffraction. **1** contains a pair of [Fe^{III}(*p*-Cl_4TPP)]$^+$ units that sandwich a [Cu^{II}(MNT)$_2$]$^{2-}$ anion; the Fe^{III} atoms are linked to the Cu^{II} atom by sulfur bridges (Fe–S = 2.482 (3) Å). A [Cu^{III}(MNT)$_2$]$^-$ anion interacts weakly with the iron atoms (Fe–S = 3.286 (4) Å). **2** also contains a pair of [Fe^{III}(*p*-Cl_4TPP)]$^+$ units sandwiching a [Cu^{II}(MNT)$_2$]$^{2-}$ anion (Fe–S = 2.472 (2) Å) and a weakly interacting [Cu^{III}(MNT)$_2$]$^-$ anion (Fe–S = 3.176 (3) Å). In both **1** and **2**, the Cu^{II} atom occupies a site of 2-fold symmetry, making the iron porphyrins structurally identical. The structure of **3** is less symmetric but also contains a pair of [Fe^{III}(*p*-Cl_4TPP)]$^+$ units sandwiching a [Cu^{II}(MNT)$_2$]$^{2-}$ anion (Fe–S = 2.444 (2), 2.549 (2) Å). In **3** the [Cu^{III}(MNT)$_2$]$^-$ anion interacts more strongly with one iron atom (Fe–S = 2.956 (2) Å) than with the other (Fe–S = 3.641 (2) Å). The metric parameters are consistent with admixed-spin (S = $^3/_2$, $^5/_2$) assignments for the iron atoms in all three compounds, as are the Mössbauer results for a mixture of **1** and **2** (δ = 0.38 mm s^{-1}, ΔE = 3.09 mm s^{-1}). The magnetic susceptibility of this mixture indicates that the iron atoms are in an intermediate spin (S = $^3/_2$) or a spin-admixed (S = $^3/_2$, $^5/_2$) state.

Introduction

The enzyme cytochrome *c* oxidase (CcO), which catalyzes the reduction of O_2 to H_2O, contains two Fe hemes and at least two Cu sites.[2] The O_2 binding site is thought to contain an Fe atom and a Cu atom in close proximity.[3] The origin of the unusual magnetic and spectroscopic properties exhibited by the resting oxidized form of the active site remains a matter of much interest. The reason(s) for the absence of an EPR signal from this Fe_{a3}–Cu_B site has been the subject of considerable speculation. In one widely accepted model, the EPR silence is thought to result from very strong ligand-mediated antiferromagnetic coupling ($-J > 200$ cm^{-1}) between the Cu(II) and the Fe(III) heme unit.[4] Another possible model involves a ligand-mediated spin-relaxation broadening between these metal centers.[5] The latter mechanism does not demand a high degree of exchange coupling between the metal centers.

Many putative model complexes for the resting, oxidized active site have been prepared. These complexes have contained various bridging ligands, including imidazolate,[6] oxygen,[7] halogens or pseudohalogens,[8] and bipyrimidyl.[9] None of these "model" complexes have exhibited antiferromagnetic coupling between the metal centers strong enough to produce EPR silence. The largest

(1) (a) Colorado State University. (b) Present address: Department of Chemistry, Otago University, Dunedin, New Zealand. (c) University of North Carolina. (d) Hiroshima University. (e) University of Vermont.
(2) Einarsdottir, O.; Caughey, W. S. *Biochem. Biophys. Res. Commun.* **1985**, *129*, 840.
(3) Malmström, B. G. In *Metal Ion Activation of Dioxygen*; Spiro, T. G., Ed.; Wiley: New York, 1980; Chapter 5.
(4) Palmer, G.; Babcock, G. T.; Vickery, L. E. *Proc. Natl. Acad. Sci. U.S.A.* **1976**, *73*, 2206.
(5) Elliott, C. M.; Akabori, K. *J. Am. Chem. Soc.* **1982**, *104*, 2671.
(6) (a) Dessens, S. E.; Merill, C. L.; Saxton, R. J.; Ilaria, R. L.; Lindsey, J. W.; Wilson, L. J. *J. Am. Chem. Soc.* **1982**, *104*, 4357. (b) Wilson, L. J.; Chunplang, V.; Lemke, B. K.; Merril, C. L.; Saxton, R. J.; Watson, M. L. *Inorg. Chim. Acta* **1983**, *79*, 107. (c) Saxton, R. J.; Wilson, L. J. *J. Chem. Soc., Chem. Commun.* **1984**, 359. (d) Cutler, A. C.; Brittain, T.; Boyd, P. D. W. *J. Inorg. Biochem.* **1985**, *24*, 199. (e) Chunplang, V.; Wilson, L. J. *J. Chem. Soc., Chem. Commun.* **1985**, 1761. (f) Brewer, C. T.; Brewer, G. *J. Inorg. Biochem.* **1986**, *26*, 247. (g) Brewer, C. T.; Brewer, G. A. *Inorg. Chem.* **1987**, *26*, 3420.
(7) (a) Gunter, M. J.; Mander, L. N.; Murray, K. S. *J. Chem. Soc., Chem. Commun.* **1981**, 799. (b) Gunter, M. J.; Mander, L. N.; Murray, K. S.; Clark, P. E. *J. Am. Chem. Soc.* **1981**, *103*, 6784. (c) Chang, C. K.; Koo, M. S.; Ward, B. *J. Chem. Soc., Chem. Commun.* **1982**, 716. (d) Lukas, B.; Miller, J. R.; Silver, J.; Wilson, M. T.; Morrison, I. E. G. *J. Chem. Soc., Dalton Trans.* **1982**, 1035. (e) Saxton, R. J.; Olson, L. W.; Wilson, L. J. *J. Chem. Soc., Chem. Commun.* **1982**, 984. (f) Journaux, Y.; Kahn, O.; Zarembowitch, J.; Galy, J.; Jaud, J. *J. Am. Chem. Soc.* **1983**, *105*, 7585. (g) Kanda, W.; Okawa, H.; Kida, S. *Bull. Chem. Soc. Jpn.* **1984**, *57*, 1159. (h) Elliott, C. M.; Jain, N. C.; Cranmer, B. K.; Hamburg, A. W. *Inorg. Chem.* **1987**, *26*, 3655.
(8) (a) Gunter, M. J.; Mander, L. N.; McLaughlin, G. M.; Murray, K. S.; Berry, K. J.; Clark, P. E.; Buckingham, D. A. *J. Am. Chem. Soc.* **1980**, *102*, 1470. (b) Berry, K. J.; Gunter, M. J.; Murray, K. S. *Nouv. J. Chim.* **1980**, *4*, 581. (c) Gunter, M. J.; Berry, K. J.; Murray, K. S. *J. Am. Chem. Soc.* **1984**, *106*, 4227.
(9) (a) Petty, R. H.; Welch, B. R.; Wilson, L. J.; Bottomly, L. A.; Kadish, K. M. *J. Am. Chem. Soc.* **1980**, *102*, 611. (b) Brewer, G. A.; Sinn, E. *Inorg. Chem.* **1984**, *23*, 2532.

0020-1669/90/1329-2663$02.50/0

Table I. Crystallographic Parameters and Refinement Results

	1	2	3
mol formula	$C_{126}H_{90}Cl_8Cu_2Fe_2N_{17}S_8$	$C_{132}H_{96}Cl_8Cu_2Fe_2N_{17}S_8$	$C_{138}H_{102}Cl_8Cu_2Fe_2N_{17}S_8$
mol wt	2621.1	2699.2	2777.3
space group	$C2/c$	$C2/c$	$P\bar{1}$
temp, °C	20	−130	−130
a, Å	17.222 (4)	17.489 (5)	13.378 (3)
b, Å	26.818 (5)	26.515 (7)	17.356 (2)
c, Å	27.497 (8)	27.006 (11)	28.918 (7)
α, deg	90	90	104.05 (2)
β, deg	103.84 (2)	101.39 (3)	99.62 (2)
γ, deg	90	90	98.38 (2)
V, Å^3	12331	12277	6299
Z	4	4	2
D(calcd), g cm^{-3}	1.41	1.46	1.46
radiation (λ, Å)	Mo Kα (0.7107)	Mo Kα (0.7107)	Mo Kα (0.7107)
μ, cm^{-1}	9.3	9.4	9.2
R	0.102	0.091	0.063
R_w	0.101	0.092	0.069

coupling, $-J = 70$ cm^{-1}, has been observed in an oxygen-bridged system.[7g]

We have synthesized model complexes involving iron porphyrins and copper complexes in which sulfur atoms link the two metals.[5,10] Systems in which sulfur acted as a bridging atom were chosen on the basis of EXAFS studies, which have suggested the presence of a third-row ligand (S or Cl) about the Fe(III) and the Cu(II) of the active site.[11,12] Herein, we discuss the preparation and characterization of three compounds involving similar sulfur-bridged species, two of which exhibit only a weak EPR signal.

Experimental Section

Materials. All solvents and reagents were purchased commercially and used as supplied except as follows. Benzene and cyclohexane were distilled under N_2 from sodium benzophenone ketyl. Fe(p-Cl_4TPP)(p-Cl_4TPP^{2-} = 5,10,15,20-tetrakis(p-chlorophenyl)porphyrinate) was prepared and purified according to published procedures.[13] (TBA)[Cu(MNT)$_2$] (TBA$^+$ = tetra-*n*-butylammonium, MNT^{2-} = *cis*-1,2-dicyanoethylenedithiolate) was prepared by dichlorodicyanobenzoquinone oxidation of (TBA)$_2$[Cu^{II}(MNT)$_2$] in CH_2Cl_2.[14]

Synthesis of (TBA){[Fe(p-Cl_4TPP)][Cu(MNT)$_2$]}$_2$·C_6H_6 (1), (TBA){[Fe(p-Cl_4TPP)][Cu(MNT)$_2$]}$_2$·2C_6H_6 (2), and (TBA){[Fe(p-Cl_4TPP)][Cu(MNT)$_2$]}$_2$·3C_6H_6 (3). The preparation of **3** has been previously described.[10b] A slightly different preparation yields a mixture of all three compounds. Fe^{II}(p-Cl_4TPP) (0.048 g, 0.060 mmol) is dissolved in benzene (70 mL) under N_2, and solid (TBA)[Cu^{III}(MNT)$_2$] (0.035 g, 0.060 mmol) is added. The reaction mixture is stirred at room temperature for 3 h and then filtered to remove (TBA)$_2$[Cu^{II}(MNT)$_2$] and undissolved (TBA)[Cu^{III}(MNT)$_2$]. Vapor diffusion of cyclohexane into the filtrate over a period of 3–4 weeks yields a mixture of solid materials: (i) the major product, an Fe/Cu/Fe trinuclear species analogous to that previously reported;[5] (ii) crystals of (TBA)$_2$[Cu^{II}(MNT)$_2$] and (TBA)[Cu^{III}(MNT)$_2$]; (iii) approximately 10% (based on Fe(p-Cl_4TPP)) yield of crystals of **1** and **2**; (iv) crystals of **3**. Crystals of **1**–**3** are morphologically similar (dark brown needles). However, crystals of **3** effloresce and shatter rapidly upon removal from the mother liquor. Due to the unstable nature of crystals of **3**, no pure bulk samples of **3** have been obtained. Hence, there is no physical data on this complex other than the crystal structure, which is here reported more fully. Crystals of **1** and **2** appear to be stable indefinitely in air. Bulk samples have been obtained by mechanical sorting. Since it is not possible to distinguish visually between crystals of **1** and **2**, the samples obtained by sorting inevitably contain a mixture.

X-ray Structure Determinations. Crystal data for **1**–**3**, together with details pertaining to the X-ray diffraction experiments, are reported in Table I. In each case, the cell constants were obtained by least-squares refinement of the setting angles obtained for 25 reflections ($2\theta_{av}$ = 18.66° for **1**, 18.57° for **2**, 14.46° for **3**) on the Nicolet R3m diffractometer.[15] The stability of **1** was monitored during data collection by measurement of the intensities of standard reflections ($2\bar{2}\bar{9}$, $40\bar{4}$, $\bar{2}2\bar{2}$) every 197 data points, as was the stability of **2** (standard reflections 200, $13\bar{6}$, $\bar{5}90$). The stability of **3** was monitored during data collection by measurement of the intensities of standard reflections (070, 008, 400) every 100 data points. Over the course of the data collections, no significant change in the intensity of any standard reflection was noted. Lorentz and polarization corrections were applied in each case.

Neutral-atom scattering factors with anomalous scattering contributions were employed for all atoms.[16] The final fractional atomic coordinates for all non-hydrogen atoms may be found in Table II (for **1**) and Table III (for **2**). Selected bond lengths and angles involving the porphyrin cores, the metal atoms, and the MNT^{2-} groups may be found in Tables IV and V. Tables of anisotropic thermal parameters, calculated hydrogen atom positions, and structure factors (observed and calculated) have been included as supplementary material. Corresponding tables for **3** may be obtained as supplementary material from our earlier report on that structure.[10b]

The structure of **1** was solved by using the direct-methods program SOLV.[15] In the final structural model for **1**, the phenyl substituents on the porphyrin macrocycles were treated as rigid hexagons (C–C = 1.39 Å) to limit the number of parameters. Anisotropic thermal parameters were used for all non-hydrogen atoms, except for those of the occluded benzene molecule. Hydrogen atoms of the porphyrin cores and the TBA$^+$ cation were included in calculated positions (C–H = 0.96 Å, U(H) = $1.2U_{iso}$(C)). At convergence (weighted least-squares refinement on F, $(\text{shift/esd})_{av} < 0.02$ over last 8 cycles) the difference Fourier synthesis was free of significant features, with maximum and minimum of 0.61 and −0.64 e Å^{-3}, respectively.

The structure of **2** was solved by placement of the heavy atoms at the coordinates from **1**. Porphyrin phenyl groups were again treated as rigid hexagons, and anisotropic thermal parameters were used for all non-hydrogen atoms, except for the occluded benzene molecules. Hydrogen atoms of the porphyrin cores and the TBA$^+$ cation were included in calculated positions (as above). At convergence (weighted least-squares refinement on F, $(\text{shift/esd})_{av} < 0.008$ over last 8 cycles) the difference Fourier synthesis was free of significant features, with maximum and minimum of 0.86 and −0.77 e Å^{-3}, respectively.

Magnetic Susceptibility. Magnetic susceptibility and magnetization data for a mixture of **1** and **2** were collected with the use of a Foner-type[17] Princeton Applied Research Model 155 vibrating-sample magnetometer (VSM). The VSM magnet (Magnion H-96), power supply (Magnion HSR-1365), and associated field control unit (Magnion FFc-4 with a Rawson-Lush Model 920 MCM rotating-coil gaussmeter) were calibrated by using procedures described earlier.[18] The VSM was calibrated with Hg[Co(NCS)$_4$].[19,20] Temperatures were measured with a

(10) (a) Serr, B. R.; Headford, C. E. L.; Elliott, C. M.; Anderson, O. P. *J. Chem. Soc., Chem. Commun.* **1988**, 92. (b) Schauer, C. K.; Akabori, K.; Elliott, C. M.; Anderson, O. P. *J. Am. Chem. Soc.* **1984**, *106*, 1127.
(11) Powers, L.; Chance, B.; Ching, Y.; Angiolillo, P. *Biophys. J.* **1981**, *34*, 465.
(12) Li, P. M.; Gelles, J.; Chan, S. I.; Sullivan, R. J.; Scott, R. A. *Biochemistry* **1987**, *26*, 2091.
(13) Collman, J. P.; Brauman, J. D.; Doxsee, K. M.; Halbert, T. R.; Bunnenbert, E.; Linder, R. E.; LaMar, G. N.; Grandio, J. D.; Lang, G.; Spartalian, K. *J. Am. Chem. Soc.* **1980**, *102*, 4182.
(14) Muetterties, E. L., Ed. *Inorganic Syntheses*; McGraw Hill: New York, 1961; Vol. X, p 13.
(15) Calculations for diffractometer operations were performed by using software supplied with the Nicolet R3m diffractometer. All structural calculations were performed with the SHELXTL program library written by G. M. Sheldrick and supplied by Nicolet XRD Corp., Madison, WI.
(16) *International Tables for X-Ray Crystallography*; Kynoch: Birmingham, England, 1974; Vol. IV, pp 99, 149.
(17) Foner, S. *Rev. Sci. Instrum.* **1959**, *30*, 548.
(18) Losee, D. B.; Hatfield, W. E. *Phys. Rev. B: Solid State* **1974**, *10*, 212.
(19) Figgis, B. N.; Nyholm, R. S. *J. Chem. Soc.* **1958**, 4190.

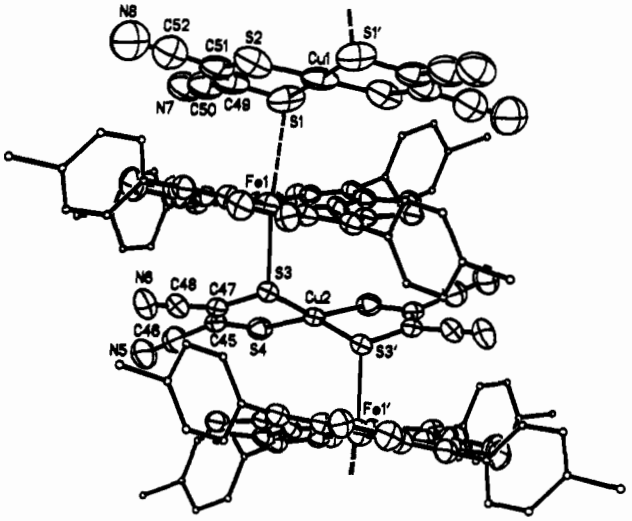

Figure 1. View of the metal-containing anionic unit of **1**. Thermal ellipsoids are drawn at the 30% probability level, carbon atoms of the phenyl rings and chlorine atoms have been drawn as spheres of arbitrary radius for clarity, and hydrogen atoms have been omitted. The numbering scheme for the MNT^{2-} ligands is shown.

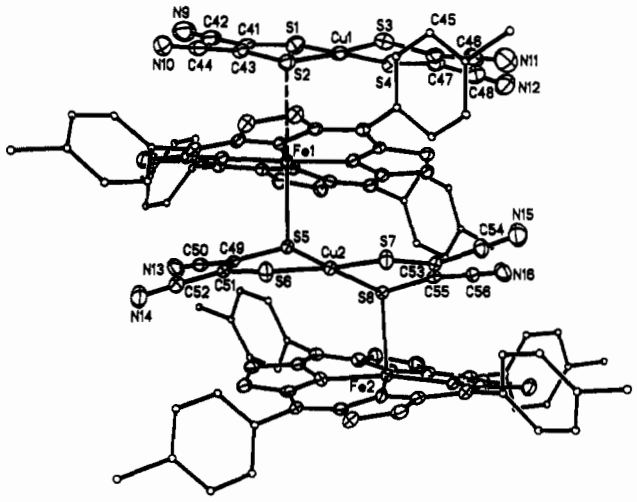

Figure 2. View of the metal-containing anionic unit of **3**. Thermal ellipsoids are drawn at the 50% probability level, carbon atoms of the phenyl rings and chlorine atoms have been drawn as spheres of arbitrary radius for clarity, and hydrogen atoms have been omitted. The numbering scheme for the MNT^{2-} ligands is shown.

calibrated GaAs diode.[21] The data were corrected for diamagnetism of the constituent atoms by using Pascal's constants,[22,23] with a diamagnetic correction for TPP^{2-} of -700×10^{-6} cgs units.[24] The sample ($\sim$100 mg) was obtained by hand selection of crystals (see above), which were ground under an inert atmosphere.

The fitting calculations were carried out by using a Simplex nonlinear least-squares fitting program,[25] with the criterion of best fit being the minimum value of the function

$$F = \sum_i \frac{[\chi_i^{obsd} T_i - \chi_i^{calc} T_i]^2}{[\chi_i^{obsd} T_i]^2} \quad (1)$$

Because of the insensitivity of the data to the parameters in the model, two sets of calculations were carried out. In one set of calculations, the quantity $\chi_i T_i$ was varied, while in the other set of calculations, only χ_i values were varied to obtain the minimum value of F. It was reasoned that parameters from both calculations must agree for them to be valid. The success of the fits (see below) confirmed this procedure.

In all calculations, g_{Cu} was held constant at 2.046, a value found for several $[Cu(MNT)_2]^{2-}$ salts.[26] The value of J_{Fe-Fe} was constrained to take on only very small values in one series of calculations, while the parameter was allowed to vary freely in other calculations. Four reasonable fits were obtained with $F < 0.015$. The parameters obtained in these calculations are listed in Table VI.

Mössbauer Spectroscopy. Mössbauer spectra for a mixture (the same mixture that was used for magnetic susceptibility measurements) of **1** and **2** were determined with a constant-acceleration spectrometer equipped with a ^{57}Co source in a Rh matrix. Magnetically perturbed spectra were obtained in longitudinally applied fields up to 8 T, with the source and absorber at 4.2 K. The isomer shifts reported are with reference to Fe metal at room temperature.

In order to extract the values of the magnetic hyperfine field parameters from the spectra, the data were fitted by a least-squares method to an electronic model based on a phenomenological spin Hamiltonian

$$\mathcal{H} = \beta \mathbf{H}(g_{xx}\mathbf{S}_x + g_{yy}\mathbf{S}_y + g_{zz}\mathbf{S}_z) \quad (2)$$

with fictitious spin $S = {}^1/_2$. The nuclear Hamiltonian was the usual

$$\mathcal{H} = -g_n\beta_n\mathbf{H}_{eff}\mathbf{I} + \mathbf{H}_Q \quad (3)$$

where $\mathbf{H}_Q$ is the quadrupole interaction and $\mathbf{H}_{eff}$ is the vector sum of the magnetic hyperfine field and applied magnetic field. The variable parameters in the calculation were the values of $g_{xx}, g_{yy}, g_{zz}, A_{xx}, A_{yy}, A_{zz}$, the quadrupole interaction parameter, and the isomer shift. Table VII contains the parameters that provided the best fit to the data.

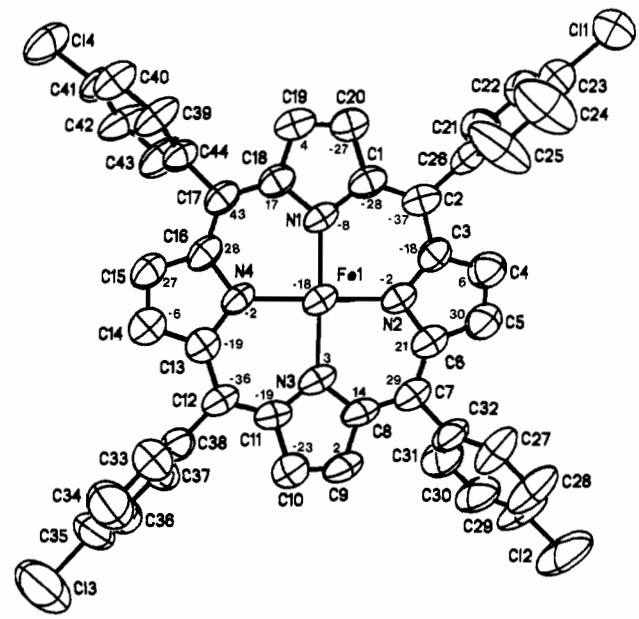

Figure 3. Numbering scheme for the $[Fe(p\text{-}Cl_4TPP)]^+$ unit of **1**, with thermal ellipsoids drawn at the 50% probability level. Also shown are the distances ($\times 10^2$ Å) above and below the best plane through the 24 atoms of the porphyrin core.

EPR Spectroscopy. Four independent samples of a mixture of **1** and **2** were obtained by hand sorting of crystals, and each was ground under an inert atmosphere. The EPR spectrum of each such solid sample was obtained on an IBM ER-200 spectrometer equipped with a variable-temperature unit. The low solubility of these compounds in noncoordinating, glass-forming solvents precluded a study of their frozen-solution EPR spectrum. Quantization of the signal was attempted by double integration of the spectrum, using $[Fe(TPP)(OSO_2CF_3)]$ as a standard.[27]

Results and Discussion

Crystal Structures of 1–3. The structures of the iron- and copper-containing units of **1** and **3** are shown in Figures 1 and 2. The structure of **2** is very similar to that of **1**, and identical numbering schemes were used for **1** and **2**.

(20) Brown, D. B.; Crawford, V. H.; Hall, J. W.; Hatfield, W. E. *J. Phys. Chem.* **1977**, *81*, 1303.
(21) Type TG-100 FPA (Special), No. 4277, Lake Shore Cryotronics, Westerville, OH.
(22) Konig, E. *Magnetic Properties of Transition Metal Compounds*; Springer-Verlag: West Berlin, 1966.
(23) Weller, R. R.; Hatfield, W. E. *J. Chem. Educ.* **1979**, *56*, 652.
(24) Eaton, G. R.; Eaton, S. S. *Inorg. Chem.* **1980**, *19*, 1095.
(25) (a) Spendley, W.; Hext, G. R.; Himsworth, F. R. *Technometrics* **1962**, *4*, 441. (b) Nedler, J. A.; Mead, R. *Comput. J.* **1965**, *7*, 308.
(26) Werden, B. G.; Billig, E.; Gray, H. B. *Inorg. Chem.* **1966**, *5*, 78.
(27) $FeTPP(O_3SCF_3)$ has a high-spin axial EPR spectrum with $g_\perp \sim 6$ and $g_\parallel \sim 2$.

Table II. Atomic Coordinates ($\times 10^4$) and Isotropic Thermal Parameters ($Å^2 \times 10^3$)[a] for **1**

atom	x	y	z	U_{iso}[b]	atom	x	y	z	U_{iso}[b]
Fe1	813 (1)	4320 (1)	8798 (1)	60 (1)*	C24	3758 (4)	2508 (3)	8809 (2)	162 (8)*
Cu1	10000	5000	5000	117 (1)*	C25	3163 (4)	2871 (3)	8745 (2)	160 (8)*
Cu2	0	3744 (1)	7500	67 (1)*	C26	2851 (4)	3013 (3)	9148 (2)	70 (4)*
S1	9412 (3)	4282 (1)	5049 (1)	134 (2)*	C27	3468 (5)	5643 (3)	9034 (3)	122 (6)*
S2	8870 (2)	5372 (1)	4721 (1)	135 (2)*	C28	4054 (5)	6012 (3)	9154 (3)	149 (8)*
S3	836 (1)	4339 (1)	7899 (1)	69 (1)*	C29	4051 (5)	6345 (3)	9544 (3)	137 (7)*
S4	1016 (2)	3219 (1)	7508 (1)	89 (1)*	C30	3462 (5)	6308 (3)	9813 (3)	120 (6)*
N1	788 (4)	3593 (2)	8902 (2)	58 (3)*	C31	2876 (5)	5940 (3)	9693 (3)	106 (5)*
N2	1980 (4)	4311 (2)	9078 (2)	62 (3)*	C32	2879 (5)	5607 (3)	9303 (3)	87 (4)*
N3	818 (4)	5055 (2)	8804 (2)	68 (3)*	C33	−1511 (4)	5594 (3)	7652 (3)	102 (5)*
N4	−374 (4)	4330 (2)	8632 (2)	59 (3)*	C34	−2078 (4)	5952 (3)	7439 (3)	130 (7)*
N5	3170 (6)	3369 (4)	7529 (4)	148 (6)*	C35	−2324 (4)	6307 (3)	7742 (3)	114 (6)*
N6	2947 (5)	4707 (4)	8070 (4)	130 (5)*	C36	−2001 (4)	6303 (3)	8258 (3)	111 (6)*
N7	7536 (7)	3650 (4)	4584 (4)	157 (6)*	C37	−1433 (4)	5946 (3)	8471 (3)	97 (5)*
N8	6743 (8)	5085 (5)	4166 (5)	201 (8)*	C38	−1188 (4)	5591 (3)	8168 (3)	71 (4)*
N9	0	211 (6)	2500	124 (7)*	C39	−1610 (4)	2746 (2)	8573 (2)	92 (5)*
Cl1	4797 (2)	1846 (1)	9365 (2)	129 (2)*	C40	−2230 (4)	2450 (2)	8658 (2)	95 (5)*
Cl2	4781 (3)	6782 (2)	9729 (2)	185 (2)*	C41	−2516 (4)	2523 (2)	9086 (2)	85 (4)*
Cl3	−3011 (3)	6757 (2)	7472 (2)	202 (3)*	C42	−2183 (4)	2893 (2)	9429 (2)	107 (6)*
Cl4	−3315 (2)	2182 (1)	9178 (1)	124 (2)*	C43	−1564 (4)	3190 (2)	9344 (2)	101 (5)*
C1	1433 (5)	3263 (3)	8963 (3)	67 (4)*	C44	−1277 (4)	3117 (2)	8916 (2)	69 (4)*
C2	2225 (5)	3405 (3)	9073 (3)	67 (4)*	C45	1808 (5)	3646 (4)	7692 (3)	79 (4)*
C3	2462 (5)	3902 (3)	9150 (3)	64 (3)*	C46	2578 (7)	3488 (5)	7605 (4)	117 (6)*
C4	3268 (6)	4049 (4)	9365 (4)	88 (5)*	C47	1751 (6)	4092 (4)	7856 (3)	77 (4)*
C5	3280 (6)	4537 (4)	9410 (4)	96 (5)*	C48	2424 (6)	4431 (4)	7969 (4)	101 (5)*
C6	2482 (5)	4718 (3)	9219 (3)	73 (4)*	C49	8441 (9)	4400 (5)	4750 (4)	115 (6)*
C7	2262 (6)	5214 (3)	9163 (3)	73 (4)*	C50	7945 (10)	3988 (6)	4665 (5)	144 (8)*
C8	1479 (6)	5368 (3)	8941 (3)	71 (4)*	C51	8220 (7)	4887 (5)	4624 (4)	120 (6)*
C9	1246 (7)	5854 (3)	8808 (4)	86 (5)*	C52	7421 (8)	4997 (5)	4370 (5)	145 (7)*
C10	468 (6)	5860 (4)	8580 (4)	87 (5)*	C60	−703 (8)	−102 (7)	2239 (7)	180 (10)*
C11	185 (5)	5362 (3)	8580 (3)	64 (4)*	C61	−443 (11)	−494 (8)	1869 (7)	204 (12)*
C12	−591 (5)	5214 (3)	8393 (3)	67 (4)*	C62	−1041 (15)	−896 (8)	1743 (12)	319 (24)*
C13	−859 (5)	4736 (3)	8444 (3)	62 (3)*	C63a	−976 (16)	−1260 (12)	1345 (14)	196 (18)*
C14	−1666 (6)	4585 (4)	8356 (3)	73 (4)*	C63b	−559 (30)	−1410 (13)	1578 (17)	154 (24)*
C15	−1681 (6)	4114 (3)	8512 (3)	73 (4)*	C64	292 (9)	538 (6)	2123 (6)	156 (9)*
C16	−875 (5)	3947 (3)	8682 (3)	66 (4)*	C65	−308 (10)	892 (6)	1820 (6)	165 (9)*
C17	−649 (5)	3461 (3)	8826 (3)	62 (3)*	C66	30 (14)	1193 (10)	1445 (8)	250 (17)*
C18	133 (5)	3292 (3)	8892 (3)	65 (4)*	C67	−533 (16)	1537 (11)	1146 (10)	360 (25)*
C19	373 (6)	2783 (3)	8950 (3)	78 (4)*	C70	0	3321 (14)	2500	300 (17)
C20	1143 (6)	2764 (3)	8972 (3)	72 (4)*	C71	−727 (15)	3076 (11)	2316 (10)	289 (12)
C21	3134 (4)	2790 (3)	9616 (2)	91 (5)*	C72	−738 (16)	2553 (12)	2326 (11)	329 (14)
C22	3729 (4)	2427 (3)	9680 (2)	96 (5)*	C73	0	2255 (15)	2500	334 (19)
C23	4041 (4)	2285 (3)	9277 (2)	91 (5)*					

[a] Estimated standard deviations in the least significant digits are given in parentheses. [b] For values with asterisks, the equivalent isotropic U is defined as one-third of the trace of the U_{ij} tensor.

All three compounds contain a neutral trinuclear $Fe^{III}/Cu^{II}/Fe^{III}$ unit, which interacts weakly with a $[Cu^{III}(MNT)_2]^-$ anion. Figures 3–5 show the numbering scheme employed for the porphyrin(s) in each case and the deviations from the best least-squares plane through the 24 atoms of each porphyrin core.

In each case, the neutral trinuclear unit consists of a pair of Fe^{III} porphyrins that sandwich a $[Cu^{II}(MNT)_2]^{2-}$ anion. This $[Cu^{II}(MNT)_2]^{2-}$ anion is bound to the Fe atoms through cis sulfur atoms, one from each of the MNT^{2-} ligands. A sulfur atom of the $[Cu^{III}(MNT)_2]^-$ anion occupies the sixth coordination site about the Fe1 atoms in **1**–**3**. In **1** and **2**, the Cu atom of the bridging $[Cu^{II}(MNT)_2]^{2-}$ anion occupies a site of crystallographic 2-fold symmetry, making the iron porphyrins structurally identical; the Cu atom of the weakly associated $[Cu^{III}(MNT)_2]^-$ anion resides at a crystallographic inversion center. The iron porphyrins and copper MNT^{2-} complexes occupy general positions in **3**.

The structural results provide unambiguous identification of the copper oxidation states in all three compounds. For $[Cu^{III}(MNT)_2]^-$, previous studies give Cu^{III}–S(av) = 2.170 (8) Å,[28] which is close to the values of Cu1–S(av) for **1** (2.18 (3) Å), **2** (2.172 (4) Å), and **3** (2.180 (3) Å). (For all averages given, the number in parentheses is the standard deviation of the sample.) For $[Cu^{II}(MNT)_2]^{2-}$, Cu^{II}–S(av) = 2.28 (2) Å,[29] a value similar to the Cu2–S(av) distances for **1** (2.246 (8) Å), **2** (2.25 (1) Å), and **3** (2.26 (1) Å).

In each case, the bridging interactions involving sulfur result in longer Cu–S bond distances to the bridging sulfur atoms and distortions from planarity for the $[Cu^{II}(MNT)_2]^{2-}$ anions. In **1**, for example, Cu2–S3(bridging) = 2.251 (2) Å and Cu2–S4(nonbridging) = 2.240 (3) Å; Cu1–S1(bridging) = 2.194 (3) Å, while Cu1–S2(nonbridging) = 2.158 (4) Å. The deviations of the S atoms from the best least-squares plane through Cu2 and the four surrounding S atoms in **1** are +0.62 Å (S3) and −0.55 Å (S4). Similar distortions occur for the bridging $[Cu^{II}(MNT)_2]^{2-}$ anions in **2** and **3**.

Clear-cut spin-state assignments for the Fe^{III} atoms are difficult to infer from the metric results alone. The Fe1 atoms in **1**–**3** exhibit weak axial interactions with sulfur atoms of the $[Cu^{II}(MNT)_2]^{2-}$ anion and very weak axial interactions with sulfur atoms of the $[Cu^{III}(MNT)_2]^-$ anion; all of these iron atoms might therefore be described as six-coordinate. Not surprisingly, given the asymmetry of these axial interactions, these Fe(III) atoms are not centered in the planes of the porphyrin nitrogen atoms but instead are displaced toward the sulfur atoms of the more strongly bound bridging $[Cu^{II}(MNT)_2]^{2-}$ anions ($Fe1–Ct_N$ = 0.18 Å for **1**, 0.17 Å for **2**, and 0.12 Å for **3**).

In six-coordinate high-spin and intermediate-spin Fe^{III} porphyrins, $Fe–Ct_N$ is generally very near zero.[30–34] However, the

(28) Forrester, J. D.; Zalkin, A.; Templeton, D. H. *Inorg. Chem.* **1964**, *3*, 1507.
(29) Plumlee, K. W.; Hoffman, B. M.; Ibers, J. A.; Soos, Z. G. *J. Chem. Phys.* **1975**, *63*, 1926.
(30) Scheidt, W. R.; Reed, C. A. *Chem. Rev.* **1981**, *81*, 543.

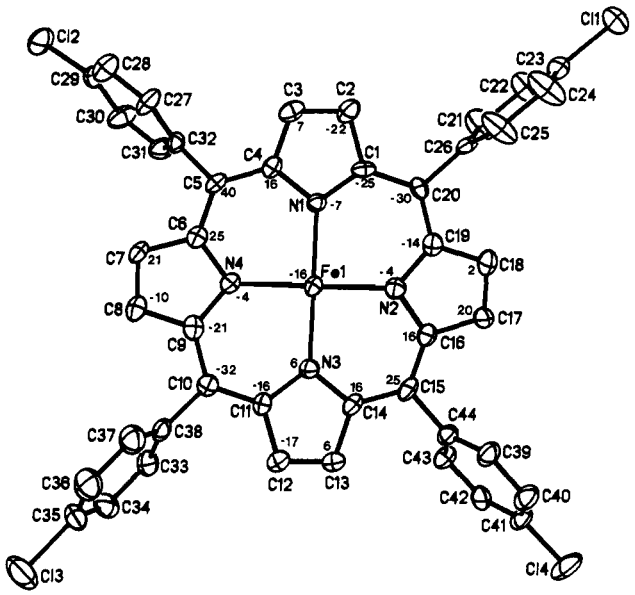

Figure 4. Numbering scheme for the $[Fe(p\text{-}Cl_4TPP)]^+$ unit of **2**, with thermal ellipsoids drawn at the 50% probability level. Also shown are the distances ($\times 10^2$ Å) above and below the best plane through the 24 atoms of the porphyrin core.

$Fe-Ct_N$ distances for **1**–**3** are outside of the range 0.00–0.09 Å characteristic of six-coordinate low-spin Fe^{III} porphyrin complexes.[30,01]

In five-coordinate Fe^{III} porphyrin complexes, the Fe atom is expected to be displaced toward the axial ligand.[30-33] Given the weak interactions with the ligand in the sixth coordination site, the Fe1 atoms in **1**–**3** are better described as five-coordinate. In fact, the $Fe-Ct_N$ distances approach values typical of five-coordinate intermediate or admixed-spin porphyrins ($Fe-Ct_N$ = 0.18–0.30 Å).[30-33] The average $Fe-N_P$ bond lengths ($Fe1-N_P$ = 1.976 (6) Å for **1**, 1.977 (6) Å for **2**, 1.98 (1) Å for **3**) are within the range found for five-coordinate intermediate or admixed-spin iron(III) porphyrin complexes ($Fe-N_P$ = 1.96–2.01 Å for $S = {}^3/_2$,[30-33] 2.05–2.09 Å for $S = {}^5/_2$[30,31,34]). The Fe2 atom in **3** is most certainly described as five-coordinate, since the Fe2···S3 distance of 3.641 (2) Å is greater than the sum (~3.2 Å) of the van der Waals radii.[35] The distances Fe2–S8 (2.444 (2) Å), $Fe2-N_P(av)$ (1.976 (7) Å), and $Fe2-Ct_N$ (0.20 Å) are consistent with an intermediate-spin assignment for Fe2. In all three complexes, the shrinking of the porphyrin core to accommodate the short $Fe-N_P$ distances is accomplished through S_4 ruffling (see Figures 3–5).

It is important to note the structural similarities between **1** and **2**. The strongly linked trinuclear $Fe^{III}/Cu^{II}/Fe^{III}$ units in these two compounds are virtually identical (for **1**, $Fe1-N_P$ = 1.976 (6) Å, Fe1–S3 = 2.482 (3) Å, $Cu2-S_{av}$ = 2.246 (8) Å, and $Fe-Ct_N$ = 0.18 Å; for **2**, $Fe1-N_P$ = 1.977 (6) Å, Fe1–S3 = 2.472 (2) Å, $Cu2-S_{av}$ = 2.25 (1) Å, and $Fe-Ct_N$ = 0.17 Å). While the bond lengths are essentially identical for the trinuclear units of **1** and **2**, the Fe–S–Cu angles differ (Fe–S–Cu = 108.0 (1)° for **1**, 105.1 (1)° for **2**), and this gives rise to a significant difference in the Fe···Cu distance (Fe···Cu = 3.833 (4) Å for **1**, 3.760 (3) Å for **2**). At the same time, the strength of the interaction with the $[Cu^{III}(MNT)_2]^-$ counterion (Fe1–S1 = 3.286 (4) Å for **1**, 3.176 (3) Å for **2**) is slightly different. As discussed above, the iron atoms in these compounds are essentially five-coordinate, so this small difference in the weak interaction with the diamagnetic $[Cu^{III}(MNT)_2]^-$ anion is not expected to cause significant differences in the physical properties of these two species.

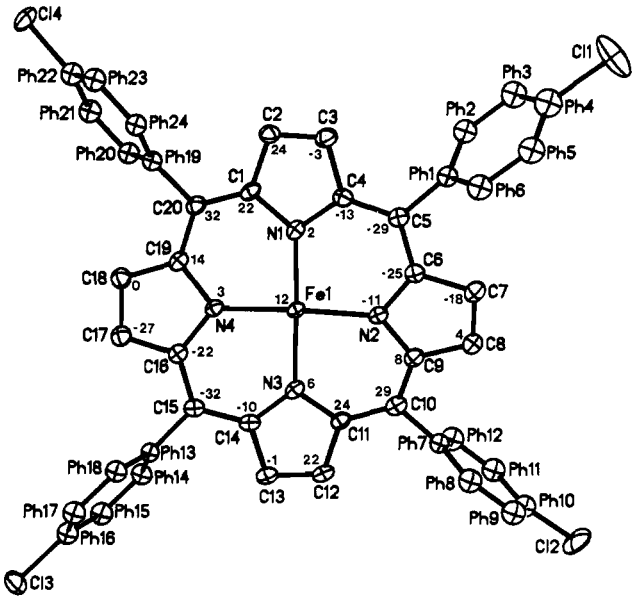

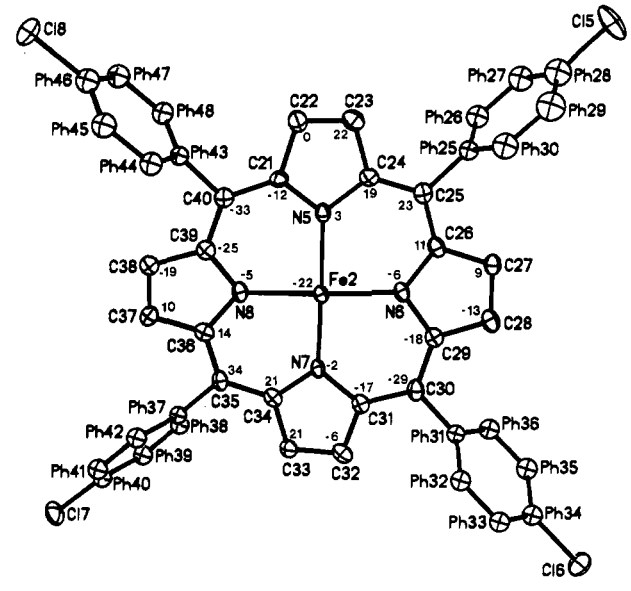

Figure 5. Numbering scheme for the $[Fe(p\text{-}Cl_4TPP)]^+$ units of **3**, with thermal ellipsoids drawn at the 50% probability level. Also shown are the distances ($\times 10^2$ Å) above and below the best plane through the 24 atoms of the porphyrin core.

Fe–S bond distances in porphyrin complexes (2.30–2.37 Å)[36] are remarkably insensitive to variations in the charge or chemical character of the sulfur atom and variations in the oxidation state, spin state, and/or coordination number of the iron atom. The Fe–S bond lengths in **1**–**3** (for **1**, Fe1–S3 = 2.482 (3) Å; for **2**, Fe1–S3 = 2.472 (2) Å; for **3**, Fe1–S5 = 2.549 (2) Å, Fe2–S8 = 2.444 (2) Å) are longer than any previously reported. These long

(31) Scheidt, W. R.; Lee, Y. J. In *Structure and Bonding, Metal Complexes with Tetrapyrrole Ligands I*; Buchler, J. W., Ed.; Springer-Verlag: Berlin, Germany, 1987; pp 1–70.
(32) Masuda, H.; Taga, T.; Osaki, K.; Sugimoto, H.; Yoshida, Z. I.; Ogoshi, H. *Bull. Chem. Soc. Jpn.* **1982**, *55*, 3891.
(33) (a) Scheidt, W. R.; Geiger, D. K.; Hayers, R. G.; Lang, G. *J. Am. Chem. Soc.* **1983**, *105*, 2625. (b) Scheidt, W. R.; Geiger, D. K.; Lee, Y. J.; Reed, C. A.; Lang, G. *Inorg. Chem.* **1987**, *26*, 1039.
(34) (a) Scheidt, W. R.; Lee, Y. J.; Geiger, D. K.; Taylor, K.; Hatano, K. *J. Am. Chem. Soc.* **1982**, *104*, 3367. (b) Scheidt, W. R.; Lee, Y. J.; Tamai, S.; Hatano, K. *J. Am. Chem. Soc.* **1983**, *105*, 778. (c) Levan, K. R.; Strouse, C. E. *Abstracts of Papers*, American Crystallographic Association Summer Meeting, Snowmass, CO, Aug 1–5, 1983. (d) Gunter, M. J.; McLaughlin, G. M.; Berry, K. J.; Murray, K. S.; Irving, M.; Clark, P. E. *Inorg. Chem.* **1984**, *23*, 283.
(35) Bondi, A. *J. Phys. Chem.* **1964**, *68*, 441.
(36) (a) Mashiko, T.; Reed, C. A.; Haller, K. J.; Kastner, M. E.; Scheidt, W. R. *J. Am. Chem. Soc.* **1981**, *103*, 5758. (b) English, D. R.; Hendrickson, D. N.; Suslick, K. S.; Eigenbrot, C. W.; Scheidt, W. R. *J. Am. Chem. Soc.* **1984**, *106*, 7258. (c) Elliott, C. M.; Akabori, K.; Anderson, O. P.; Schauer, C. K.; Hatfield, W. E.; Sczaniecki, P. B.; Mitra, S.; Spartalian, K. *Inorg. Chem.* **1986**, *25*, 1891.

Table III. Atomic Coordinates ($\times 10^4$) and Isotropic Thermal Parameters ($Å^2 \times 10^3$)[a] for **2**

atom	x	y	z	U_{iso}[b]	atom	x	y	z	U_{iso}[b]
Fe1	763 (1)	4376 (1)	8782 (1)	20 (1)*	C28	−2239 (3)	2492 (2)	8640 (2)	37 (3)*
Cu1	0	5000	5000	27 (1)*	C29	−2507 (3)	2554 (2)	9090 (2)	35 (3)*
Cu2	0	3871 (1)	7500	26 (1)*	C30	−2149 (3)	2903 (2)	9448 (2)	39 (3)*
S1	−608 (1)	4296 (1)	5069 (1)	37 (1)*	C31	−1523 (3)	3190 (2)	9357 (2)	35 (3)*
S2	−1083 (1)	5400 (1)	4727 (1)	35 (1)*	C32	−1255 (3)	3129 (2)	8908 (2)	23 (2)*
S3	817 (1)	4426 (1)	7875 (1)	26 (1)*	C33	−1454 (3)	6025 (2)	8520 (1)	34 (3)*
S4	992 (1)	3274 (1)	7521 (1)	36 (1)*	C34	−1995 (3)	6394 (2)	8318 (1)	39 (3)*
N1	761 (3)	3633 (2)	8874 (2)	21 (2)*	C35	−2310 (3)	6399 (2)	7802 (1)	46 (3)*
N2	1902 (3)	4377 (2)	9028 (2)	23 (2)*	C36	−2084 (3)	6035 (2)	7487 (1)	49 (3)*
N3	748 (3)	5121 (2)	8810 (2)	23 (2)*	C37	−1543 (3)	5666 (2)	7688 (1)	40 (3)*
N4	−389 (3)	4372 (2)	8633 (2)	21 (2)*	C38	−1228 (3)	5661 (2)	8205 (1)	28 (2)*
N5	−2490 (5)	3681 (4)	4577 (3)	61 (3)*	C39	3257 (3)	5796 (2)	8914 (2)	35 (3)*
N6	−3108 (4)	5164 (3)	4110 (3)	55 (3)*	C40	3809 (3)	6180 (2)	9029 (2)	38 (3)*
N7	3104 (4)	3423 (4)	7484 (3)	61 (3)*	C41	3844 (3)	6468 (2)	9465 (2)	36 (3)*
N8	2890 (4)	4783 (3)	7984 (3)	45 (3)*	C42	3326 (3)	6373 (2)	9786 (2)	36 (3)*
N9	0	223 (4)	2500	30 (3)*	C43	2774 (3)	5990 (2)	9671 (2)	31 (3)*
Cl1	4743 (1)	1927 (1)	9403 (1)	54 (1)*	C44	2739 (3)	5701 (2)	9236 (2)	26 (2)*
Cl2	−3331 (1)	2239 (1)	9176 (1)	48 (1)*	C45	−1547 (5)	4438 (3)	4761 (3)	35 (3)*
Cl3	−2971 (2)	6856 (1)	7558 (1)	70 (1)*	C46	−2083 (5)	4014 (4)	4660 (3)	45 (3)*
Cl4	4549 (1)	6919 (1)	9628 (1)	56 (1)*	C47	−1756 (4)	4906 (3)	4612 (3)	32 (3)*
C1	1391 (4)	3315 (3)	8934 (3)	23 (2)*	C48	−2515 (5)	5044 (4)	4346 (3)	41 (3)*
C2	1145 (4)	2798 (3)	8937 (3)	31 (3)*	C49	1776 (4)	3685 (3)	7667 (3)	34 (3)*
C3	362 (4)	2817 (3)	8912 (3)	28 (3)*	C50	2516 (5)	3532 (4)	7571 (3)	42 (3)*
C4	124 (4)	3327 (3)	8866 (3)	24 (2)*	C51	1714 (4)	4166 (3)	7814 (3)	28 (3)*
C5	−654 (4)	3488 (3)	8814 (3)	23 (2)*	C52	2375 (4)	4501 (4)	7913 (3)	38 (3)*
C6	−880 (4)	3976 (3)	8676 (3)	23 (2)*	C60	321 (4)	545 (3)	2127 (3)	38 (3)*
C7	−1675 (4)	4129 (3)	8519 (3)	24 (2)*	C61	−242 (5)	911 (4)	1810 (3)	45 (3)*
C8	−1666 (4)	4624 (3)	8376 (3)	27 (2)*	C62	147 (5)	1209 (4)	1465 (4)	58 (4)*
C9	−871 (4)	4774 (3)	8458 (3)	26 (2)*	C63	−406 (8)	1549 (5)	1134 (5)	94 (6)*
C10	−635 (4)	5271 (3)	8419 (3)	24 (2)*	C64	−669 (4)	−98 (3)	2232 (4)	41 (3)*
C11	122 (4)	5431 (3)	8597 (3)	26 (2)*	C65	−438 (5)	−498 (4)	1882 (3)	43 (3)*
C12	377 (4)	5935 (3)	8606 (3)	35 (3)*	C66	−1104 (5)	−870 (4)	1720 (5)	61 (4)*
C13	1142 (4)	5942 (3)	8813 (3)	33 (3)*	C67	−881 (6)	−1302 (4)	1421 (4)	61 (4)*
C14	1374 (4)	5435 (3)	8932 (3)	24 (2)*	C70	0	3322 (12)	2500	90 (9)
C15	2146 (4)	5290 (3)	9113 (3)	28 (3)*	C71	−666 (12)	3014 (9)	2266 (9)	77 (7)
C16	2372 (4)	4795 (3)	9155 (3)	24 (2)*	C72	−641 (13)	2469 (9)	2218 (10)	84 (8)
C17	3161 (4)	4629 (3)	9313 (3)	30 (3)*	C73	0	2244 (21)	2500	175 (20)
C18	3175 (4)	4128 (3)	9282 (3)	34 (3)*	C70b	826 (12)	2719 (8)	2563 (9)	30 (7)
C19	2392 (4)	3973 (3)	9102 (3)	25 (2)*	C71b	364 (13)	3222 (9)	2494 (10)	45 (8)
C20	2168 (4)	3467 (3)	9036 (3)	22 (2)*	C72b	304 (17)	2286 (11)	2413 (14)	70 (11)
C21	3042 (3)	2868 (2)	9601 (2)	48 (3)*	C80	370 (8)	216 (6)	−360 (6)	41 (4)
C22	3643 (3)	2514 (2)	9689 (2)	45 (3)*	C81	21 (8)	533 (5)	−17 (6)	48 (4)
C23	3996 (3)	2359 (2)	9295 (2)	40 (3)*	C82	−333 (8)	315 (6)	294 (6)	53 (4)
C24	3748 (3)	2558 (2)	8811 (2)	60 (4)*	C80b	−347 (12)	113 (9)	389 (8)	18 (7)
C25	3147 (3)	2912 (2)	8723 (2)	55 (4)*	C81b	−127 (15)	472 (10)	131 (11)	37 (8)
C26	2794 (3)	3067 (2)	9117 (2)	23 (2)*	C82b	−229 (16)	−433 (12)	241 (11)	37 (8)
C27	−1613 (3)	2780 (2)	8549 (2)	35 (3)*					

[a] Estimated standard deviations in the least significant digits are given in parentheses. [b] For values with asterisks, the equivalent isotropic U is defined as one-third of the trace of the $\mathbf{U}_{ij}$ tensor.

Fe^{III}–S bonds result from the bridging character of the sulfur atom, since a similar ligand in a nonbridging mode (in (μ-FNT-*S*,*S'*)[Fe(TPP)]$_2$, where FNT^{2-} = *trans*-1,2-dicyanoethylenedithiolate)[36c] exhibits "normal" Fe^{III}–S bond lengths (2.324 (2) Å). The Fe^{III}–S bond lengths in **1**–**3** also are influenced by the presence of a sulfur ligand in the sixth coordination site of the Fe atoms; shorter Fe–S bonds to the $[Cu^{III}(MNT)_2]^-$ anion are accompanied by longer Fe–S bonds to the $[Cu^{II}(MNT)_2]^{2-}$ anion.

The Fe–S bond lengths in **1**–**3** approach the value of 2.60 Å suggested by an Fe EXAFS study of the active site of CcO.[11] The Cu–S(bridging) bond lengths (Cu2–S3 = 2.251 (2) Å in **1**, 2.260 (2) Å in **2**; Cu2–S5 = 2.261 (1) Å, Cu2–S8 = 2.278 (2) Å in **3**) are close to the Cu–S(C1) distances of 2.3 Å reported in Cu EXAFS studies on CcO depleted on the EPR-detectable copper (Cu_A).[12] The Fe–Cu distances (Fe–Cu = 3.833 (4) Å in **1**, 3.760 (3) Å in **2**, 3.858 (2) and 3.921 (2) Å in **3**) are similar to the value of 3.75 Å from Fe and Cu EXAFS studies on CcO.[11]

Magnetic Susceptibility. In order to theoretically analyze the magnetic susceptibility results for the mixture of **1** and **2**, it is necessary to postulate spin states for the iron(III) atoms. Crystallographic symmetry and structural similarities demand that the spin states of the iron(III) atoms in **1** and **2** must be identical, and the metric parameters suggest that these are either intermediate spin ($S = {}^3/_2$) or spin-admixed ($S = {}^3/_2, {}^5/_2$) states. The high-temperature magnetic moment can also be used to assign the spin states of the individual atoms. Limiting spin-only values for μ_{eff} are given by

$$\mu_{eff}^{s.o.} = [\sum_s [(4S)(S+1)]]^{1/2} \quad (4)$$

The possibilities for the spin states of the trinuclear unit $Fe^{III}/Cu^{II}/Fe^{III}$ are limited to ($^1/_2, {}^1/_2, {}^1/_2$), ($^3/_2, {}^1/_2, {}^3/_2$), or ($^5/_2, {}^1/_2, {}^5/_2$). These spin states have limiting spin-only magnetic moments of 3.00, 5.74, and 8.54 μ_B, respectively. An admixed spin state for the iron atoms ($S = {}^3/_2, {}^5/_2$) would result in a value between the latter two. The value of μ_{eff} for the mixture of **1** and **2** levels off above 30 K at ~6.2 μ_B (see Figure 6), and therefore an assignment of ($^3/_2, {}^1/_2, {}^3/_2$) for the spin-state array, with a minor $S = {}^5/_2$ spin-admixture for the iron atoms, seems most reasonable.

The theory necessary for the analysis of the magnetic susceptibility data for an M_2M' trinuclear unit[37] has been applied to analogous $Fe^{III}/Cu^{II}/Fe^{III}$ compounds.[38] With Fe1 represented by $\mathbf{S}_1$, Fe1′ by $\mathbf{S}_2$, and Cu2 by $\mathbf{S}_3$, and with

(37) Blake, A. B.; Yavari, A.; Hatfield, W. E.; Sethulekshmi, C. N. *J. Chem. Soc., Dalton Trans.* **1985**, 2509.
(38) Hatfield, W. E.; Elliott, C. M.; Ensling, J.; Akabori, K. *Inorg. Chem.* **1987**, *26*, 1930.

$$S_{12} = S_1 + S_2 \quad (5)$$

$$S = S_{12} + S_3 \quad (6)$$

the exchange and Zeeman Hamiltonians can be written as

$$H_{ex} = -2J_{12}S_1 \cdot S_2 - 2J_3 S_{12} \cdot S_3 \quad (7)$$

and

$$H_H = \mu_B(g_1 S_{12} + g_3 S_3) \cdot H \quad (8)$$

The zero-field energies and first- and second-order Zeeman coefficients were substituted into the Van Vleck equation, which was modified with a mean-field correction to account for deviations arising from intercluster interactions. The resulting corrected magnetic susceptibility expression is of the form

$$\chi_i^{cor} = \frac{\chi_i^{cluster}}{(1 - 2zJ'\chi_i^{cluster})/N\mu_b^2 g^2} \quad (9)$$

The g values for iron(III) in the four reasonable fits (Table VI) fall within a range (2.18–2.24) characteristic of intermediate-spin ferric porphyrins.[39] All four sets of parameters resulting from the best-fit calculations are reasonable, but without magneto-structural results for a series of analogous compounds, and resulting magneto-structural correlations, it is difficult to select the most appropriate magnetic parameters. To gain insight into which set of parameters is best, an atomic orbital model is helpful.

Consider the occupation of the d orbitals by electrons on both the Cu and Fe sites on the basis of simple ligand field arguments. The unpaired electron on Cu(II) lies in the $d_{x^2-y^2}$ orbital, while the electronic configuration of Fe(III) is $(d_{xz,yz})^3(d_{xy})^1(d_{z^2})^1$. On the basis of the available orbitals for superexchange, the unpaired spin in the d_{xy} orbital on Fe(III) is not expected to interact with the unpaired spin on Cu(II). However, superexchange can occur between the unpaired electrons in the Fe(III) out-of-plane orbitals and the unpaired electron on Cu(II). The possible pairwise interactions are d_{z^2}(Fe)–$d_{x^2-y^2}$(Cu), d_{xz}(Fe)–$d_{x^2-y^2}$(Cu), and d_{yz}(Fe)–$d_{x^2-y^2}$(Cu). The last two are expected to make a very small contribution to the exchange owing to the large Cu–Fe distances in **1** and **2**. The d_{z^2}(Fe)–$d_{x^2-y^2}$(Cu) interaction can be readily mediated by the bridging sulfur p orbitals bound equatorially to Cu(II) and axially to Fe(III). Sulfur is known to provide an excellent pathway for superexchange,[40] with the sign and magnitude of the exchange constant dependent on the M–L–M′ bridging angle.[41] As a general rule, the more obtuse the bridging angle, the more antiferromagnetic is the exchange coupling. In the present case, the Fe1–S3–Cu2 angle is 108.0 (1)° for **1**, and 105.1 (1)° for **2**, suggesting a small degree of antiferromagnetic character in the two compounds.

Since the structures involve extended chains, there are two possible Fe1–Fe1′ interactions, one within the strongly linked trinuclear unit and the second between trinuclear units (propagated through orbitals of the Cu(III) units). In all cases, superexchange must occur via S–Cu–S multiatom bridges. All Fe–Cu distances along the chains are large compared to the sum of the Fe(III) and Cu(III,II) ionic radii, so the orbital overlap that is crucial for exchange along the most direct pathway (d_{xz}(Fe1)–$d_{x^2-y^2}$(Cu2)–d_{xz}(Fe1′)) is likely to be small. The Fe1–Fe1′ interaction by way of the S1–Cu1–S1′ pathway is also expected to be small, due to the large Fe–S bond distances and the empty $d_{x^2-y^2}$ orbital on Cu(III). In our treatment, any chain effects will be absorbed in J' in the mean-field correction described above.

Fits a and d can be eliminated, since a ferromagnetic interaction would not be expected in view of the large Fe–S–Cu angles and the antiferromagnetic exchange found in related compounds.[39]

Table IV. Selected Bond Lengths (Å)[a] and Angles (deg)[a] for **1**

Cu1–S1	2.194 (3)	C3–C4	1.428 (12)	N4–C16	1.369 (11)
Cu1–S2	2.158 (4)	C4–C5	1.315 (15)	C16–C17	1.392 (11)
S1–C49	1.707 (14)	C5–C6	1.433 (13)	C17–C18	1.392 (13)
C49–C50	1.382 (21)	N2–C6	1.390 (10)	N1–C18	1.383 (11)
N7–C50	1.136 (19)	C6–C7	1.383 (13)	C18–C19	1.423 (12)
S2–C51	1.694 (13)	C7–C8	1.403 (13)	C19–C20	1.314 (15)
C49–C51	1.381 (18)	N3–C8	1.392 (11)	C1–C20	1.432 (12)
C51–C52	1.416 (17)	C8–C9	1.384 (12)	Fe1–S3	2.482 (3)
N8–C52	1.193 (18)	C9–C10	1.337 (15)	Cu2–S3	2.251 (2)
S1–Fe1	3.286 (4)	C10–C11	1.423 (13)	Cu2–S4	2.240 (3)
Fe1–N1	1.971 (6)	N3–C11	1.387 (10)	S3–C47	1.740 (10)
Fe1–N2	1.973 (6)	C11–C12	1.371 (12)	C47–C48	1.447 (15)
Fe1–N3	1.973 (6)	C12–C13	1.381 (12)	N6–C48	1.146 (14)
Fe1–N4	1.985 (6)	N4–C13	1.393 (10)	S4–C45	1.760 (10)
N1–C1	1.398 (11)	C13–C14	1.411 (13)	C45–C47	1.290 (16)
C1–C2	1.378 (13)	C14–C15	1.336 (13)	C45–C46	1.466 (16)
C2–C3	1.396 (12)	C15–C16	1.426 (12)	N5–C46	1.133 (16)
N2–C3	1.360 (10)				

S1–Cu1–S2	92.1 (1)	S1′–Cu1–S2	87.9 (1)
Cu1–S1–C49	102.8 (5)	Cu1–S2–C51	102.0 (4)
S1–C49–C50	115.4 (10)	S1–C49–C51	118.4 (10)
S2–C51–C49	123.6 (10)	S2–C51–C52	116.5 (9)
C49–C51–C52	119.8 (12)	C49–C50–N7	178.5 (17)
C51–C49–C50	126.2 (13)	C51–C52–N8	178.4 (16)
Cu1–S1–Fe1	101.3 (1)	C49–S1–Fe1	97.5 (5)
S1–Fe1–N1	79.5 (2)	S1–Fe1–N2	88.1 (2)
S1–Fe1–N3	91.3 (2)	S1–Fe1–N4	82.5 (2)
N1–Fe1–N2	89.2 (2)	N1–Fe1–N3	170.9 (3)
N1–Fe1–N4	89.5 (2)	N2–Fe1–N3	90.4 (3)
N2–Fe1–N4	170.6 (3)	N3–Fe1–N4	89.4 (3)
Fe1–N1–C1	126.8 (5)	Fe1–N1–C18	128.3 (5)
Fe1–N2–C3	126.6 (5)	Fe1–N2–C6	127.4 (5)
Fe1–N3–C8	127.4 (5)	Fe1–N3–C11	126.0 (5)
Fe1–N4–C13	126.1 (5)	Fe1–N4–C16	127.2 (5)
N1–C1–C2	124.6 (7)	N1–C1–C20	108.9 (8)
N1–C18–C17	125.0 (8)	N1–C18–C19	109.5 (9)
C1–N1–C18	104.7 (6)	C1–C2–C3	122.4 (8)
C2–C3–C4	123.1 (8)	N2–C3–C2	126.9 (7)
N2–C3–C4	109.7 (7)	N2–C6–C5	108.4 (8)
N2–C6–C7	126.1 (8)	C3–N2–C6	105.9 (6)
C3–C4–C5	107.7 (9)	C4–C5–C6	108.1 (9)
C5–C6–C7	125.5 (8)	C6–C7–C8	122.8 (8)
N3–C8–C7	125.4 (7)	N3–C8–C9	109.2 (8)
N3–C11–C10	108.9 (7)	N3–C11–C12	125.9 (7)
C8–N3–C11	105.5 (6)	C7–C8–C9	125.3 (9)
C8–C9–C10	109.3 (9)	C9–C10–C11	107.0 (8)
C10–C11–C12	125.1 (8)	C11–C12–C13	123.4 (7)
N4–C13–C12	125.2 (8)	N4–C13–C14	108.5 (7)
N4–C16–C15	108.6 (7)	N4–C16–C17	126.3 (8)
C13–N4–C16	106.6 (6)	C12–C13–C14	126.0 (8)
C13–C14–C15	108.0 (8)	C14–C15–C16	108.0 (8)
C15–C16–C17	124.8 (8)	C16–C17–C18	122.6 (8)
C17–C18–C19	125.0 (9)	C18–C19–C20	107.8 (8)
C19–C20–C1	108.3 (8)	C20–C1–C2	125.8 (8)
S3–Fe1–N1	99.9 (2)	S3–Fe1–N2	97.6 (2)
S3–Fe1–N3	89.3 (2)	S3–Fe1–N4	91.8 (2)
Fe1–S3–Cu2	108.0 (1)	Fe1–S3–C47	106.9 (3)
S3–Cu2–S3′	89.7 (1)	S3–Cu2–S4	91.9 (1)
S3′–Cu2–S4	149.0 (1)	S4–Cu2–S4′	102.2 (2)
Cu2–S3–C47	100.5 (4)	Cu2–S4–C45	98.3 (4)
S3–C47–C45	121.4 (8)	S3–C47–C48	116.0 (8)
S4–C45–C46	115.7 (8)	S4–C45–C47	125.8 (8)
C45–C46–N5	178.9 (12)	C45–C47–C48	122.3 (10)
C47–C48–N6	177.8 (13)	C47–C45–C46	118.2 (10)

[a] Estimated standard deviations in the least significant digits are given in parentheses.

The only fits consistent with the preceding discussion are b and c, and the inability to fit $\chi_i T_i$ (as well as χ_i) eliminates fit b. Magnetic susceptibility and μ_{eff} data are plotted in Figure 6, along with the best-fit curves using parameters from fit c. The limitations of the model employed have been discussed elsewhere.[39] Given that the measurements were conducted on a mixture of **1** and **2**, these results represent an average for the two compounds. The goodness of fit of model c to the magnetic susceptibility data supports the conclusion from the structural data that the physical

(39) Konig, E.; Konig, G. In *Landolt-Bornstein Numerical Data and Fundamental Relationships in Science and Technology, New Series*; Springer-Verlag: New York, 1976; II/8.
(40) Vincente, R.; Ribas, J.; Alvarez, S.; Segui, A.; Verdaguer, M. *Inorg. Chem.* **1987**, *26*, 4004.
(41) McGregor, K. T.; Watkins, N. T.; Lewis, D. L.; Drake, R. F.; Hodgson, D. J.; Hatfield, W. E. *Inorg. Nucl. Chem. Lett.* **1973**, *9*, 423.

Table V. Selected Bond Lengths (Å)[a] and Angles (deg)[a] for **2**

Cu1–S1	2.175 (2)	N1–C4	1.374 (9)	N2–C16	1.384 (9)
Cu1–S2	2.169 (2)	C4–C5	1.407 (10)	C16–C17	1.430 (10)
S1–C45	1.730 (8)	C5–C6	1.385 (10)	C17–C18	1.333 (11)
C45–C46	1.454 (13)	N4–C6	1.374 (9)	C18–C19	1.420 (10)
N5–C46	1.129 (13)	C6–C7	1.430 (9)	N2–C19	1.362 (9)
S2–C47	1.749 (8)	C7–C8	1.370 (11)	C19–C20	1.398 (10)
C45–C47	1.332 (12)	C8–C9	1.421 (10)	C1–C20	1.393 (10)
C47–C48	1.427 (10)	N4–C9	1.384 (9)	Fe1–S3	2.472 (2)
N6–C48	1.149 (10)	C9–C10	1.390 (11)	Cu2–S3	2.260 (2)
S1–Fe1	3.176 (3)	C10–C11	1.382 (9)	Cu2–S4	2.246 (2)
Fe1–N1	1.985 (6)	N3–C11	1.400 (9)	S3–C51	1.751 (8)
Fe1–N2	1.971 (5)	C11–C12	1.407 (11)	C51–C52	1.440 (11)
Fe1–N3	1.978 (6)	C12–C13	1.345 (10)	N8–C52	1.157 (11)
Fe1–N4	1.975 (5)	C13–C14	1.423 (10)	S4–C49	1.735 (8)
N1–C1	1.372 (9)	N3–C14	1.363 (9)	C49–C51	1.348 (12)
C1–C2	1.437 (11)	C14–C15	1.396 (10)	C49–C50	1.427 (12)
C2–C3	1.359 (11)	C15–C16	1.368 (11)	N7–C50	1.137 (12)
C3–C4	1.412 (11)				

S1–Cu1–S2	92.3 (1)	S1′–Cu1–S2	87.7 (1)
Cu1–S1–C45	101.8 (3)	Cu1–S2–C47	101.9 (3)
S1–C45–C46	115.9 (6)	S1–C45–C47	121.8 (6)
S2–C47–C45	120.6 (6)	S2–C47–C48	115.1 (7)
C45–C47–C48	124.3 (8)	C45–C46–N5	178.6 (10)
C47–C45–C46	122.3 (7)	C47–C48–N6	176.2 (10)
Cu1–S1–Fe1	99.4 (1)	C45–S1–Fe1	101.5 (3)
S1–Fe1–N1	87.3 (2)	S1–Fe1–N2	87.4 (2)
S1–Fe1–N3	91.4 (2)	S1–Fe1–N4	85.3 (2)
N1–Fe1–N2	89.2 (2)	N1–Fe1–N3	170.3 (3)
N1–Fe1–N4	89.6 (2)	N2–Fe1–N3	90.3 (2)
N2–Fe1–N4	172.2 (3)	N3–Fe1–N4	89.5 (2)
Fe1–N1–C1	127.1 (5)	Fe1–N1–C4	127.3 (5)
Fe1–N2–C16	126.6 (5)	Fe1–N2–C19	127.8 (5)
Fe1–N3–C11	126.0 (4)	Fe1–N3–C14	127.1 (5)
Fe1–N4–C6	128.0 (5)	Fe1–N4–C9	126.4 (5)
N1–C1–C2	110.7 (6)	N1–C1–C20	125.1 (6)
N1–C4–C3	109.9 (6)	N1–C4–C5	126.0 (7)
C1–N1–C4	105.5 (6)	C1–C2–C3	105.3 (7)
C2–C3–C4	108.4 (7)	C3–C4–C5	124.1 (7)
C4–C5–C6	121.9 (7)	C5–C6–C7	123.5 (7)
N4–C6–C5	126.0 (6)	N4–C6–C7	110.3 (6)
N4–C9–C8	110.4 (6)	N4–C9–C10	125.9 (6)
C6–N4–C9	105.6 (5)	C6–C7–C8	106.8 (6)
C7–C8–C9	106.9 (6)	C8–C9–C10	123.4 (7)
C9–C10–C11	122.9 (6)	N3–C11–C10	125.4 (7)
N3–C11–C12	109.4 (6)	N3–C14–C13	110.1 (6)
N3–C14–C15	126.2 (7)	C11–N3–C14	105.4 (6)
C10–C11–C12	125.2 (7)	C11–C12–C13	101.9 (7)
C12–C13–C14	107.2 (7)	C13–C14–C15	123.5 (7)
C14–C15–C16	122.5 (7)	N2–C16–C15	126.8 (6)
N2–C16–C17	108.6 (6)	N2–C19–C18	111.0 (6)
N2–C19–C20	125.6 (6)	C16–N2–C19	105.5 (5)
C15–C16–C17	124.5 (7)	C16–C17–C18	108.5 (6)
C17–C18–C19	106.4 (7)	C18–C19–C20	123.3 (7)
C19–C20–C1	122.8 (6)	C20–C1–C2	123.8 (6)
S3–Fe1–N1	100.4 (2)	S3–Fe1–N2	95.7 (2)
S3–Fe1–N3	89.3 (2)	S3–Fe1–N4	92.1 (2)
Fe1–S3–Cu2	105.1 (1)	Fe1–S3–C51	106.4 (3)
S3–Cu2–S3′	88.7 (1)	S3–Cu2–S4	91.7 (1)
S3′–Cu2–S4	152.4 (1)	S4–Cu2–S4′	100.3 (1)
Cu2–S3–C51	100.1 (3)	Cu2–S4–C49	100.1 (3)
S3–C51–C49	121.8 (6)	S3–C51–C52	116.2 (6)
S4–C49–C51	123.7 (6)	S4–C49–C50	119.0 (7)
C49–C50–N7	177.7 (10)	C49–C51–C52	122.0 (7)
C51–C52–N8	177.7 (9)	C51–C49–C50	116.9 (8)

[a] Estimated standard deviations in the least significant digits are given in parentheses.

properties of these two compounds must be very similar. The magnetic susceptibility measurements support the intermediate spin state assignments for the Fe atoms and show that there is only small antiferromagnetic coupling between the metal centers in these complexes.

Mössbauer Spectra. Figure 7 shows Mössbauer spectra of a mixture of **1** and **2** at 4.2 K in 8 T (top) and 6 T (bottom) magnetic fields. No evidence of two inequivalent iron sites is seen in any of the spectra (zero field or applied field), indicating either

Table VI. Magnetic Susceptibility Fit Parameters for a Mixture of **1** and **2**

	J_{Fe-Fe}, cm^{-1}	J_{Fe-Cu}, cm^{-1}	g_{Fe}	g_{Cu}	zJ', cm^{-1}	fit
a	0	3.618	2.181	2.046	−0.153	χ
b	0	−1.015	2.234	2.046	-6.44×10^{-3}	χ
c	−1.290	−2.102	2.173	2.046	0.309	χ, χT
d	−0.099	3.564	2.188	2.046	−0.146	χ, χT

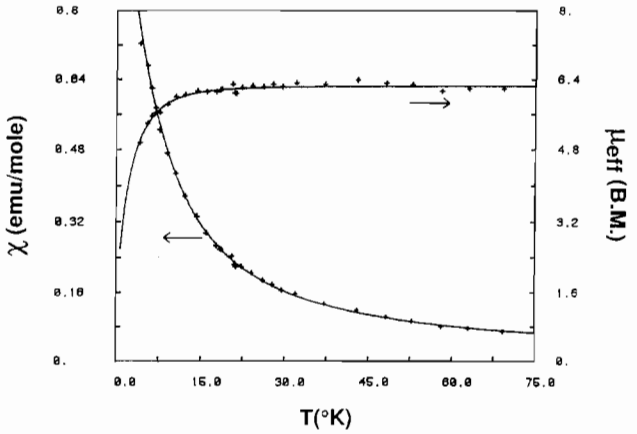

Figure 6. Molar magnetic susceptibility (χ) and effective magnetic moment (μ_{eff}) vs temperature for the mixture of **1** and **2**.

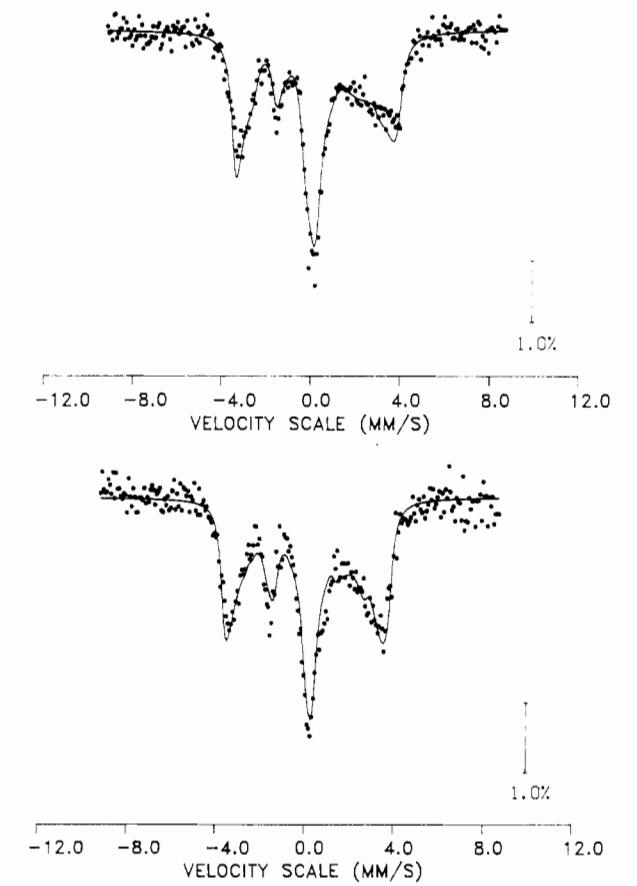

Figure 7. Mössbauer spectra of a mixture of **1** and **2** at 4.2 K in longitudinally applied magnetic fields of 8 T (top) and 6 T (bottom). The solid lines show the results of a least-squares calculation (see text for details). Vertical bars indicate 1% absorption.

that the two compounds, **1** and **2**, are extremely similar (as argued previously) or that one of the compounds is present in such small quantities as to be undetectable. Furthermore, the two spectral profiles are nearly identical, indicating that (a) a single electronic state gives rise to these spectra and (b) the spin of this state is

Table VII. Mössbauer Parameters for Iron(III) Porphyrin Complexes at 4.2 K

complex	**1** and **2**	$FeTPP(ClO_4)$	$FeOEP(ClO_4)$	$(FeTPP)_2FNT$	$FeTPP(Im)_2Cl$
ref	present work	42	43	36c	44
spin S		$^3/_2$	$^3/_2$	$^5/_2$	$^1/_2$
isomer shift δ, mm/s	0.38	0.39	0.37	0.41	0.23
quadrupole splitting ΔE, mm/s	3.09	3.50	3.57	0.80	2.23
line width Γ, mm/s	0.5	0.3	0.3		
asym param η	0.0	0.0	0.0		
g	1.7, 2.6, 2.0				
H_{int}, T[a]	−17.0, −22.7, +5.5	−20.9, −22.4, +0.9			

[a] Negative fields oppose the applied field.

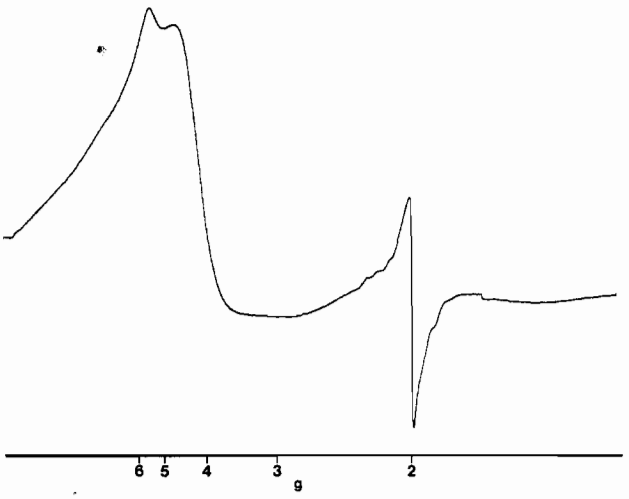

Figure 8. EPR spectrum of the mixture of **1** and **2**. Experimental conditions: powdered sample, 5.3 K, 10-mW power, 9.216-GHz microwave frequency, 1.6-G modulation amplitude, 2×10^3 gain.

saturated at these two values of applied field.

The parameters for the mixture of **1** and **2** obtained by least-squares fit are listed in Table VII, along with the parameters for other Fe(III) porphyrin complexes. The parameters for **1** and **2** are similar to those obtained for the monomeric complexes $[FeTPP(ClO_4)]$[42] and $[FeOEP(ClO_4)]$,[43] both of which have a spin state $S = {}^3/_2$. In particular, the results for our sample compare well with those for $FeTPP(ClO_4)$; the isomer shifts are identical, the quadrupole splittings are similar in size, and the magnetic hyperfine interaction shows the same anisotropy (relatively large internal field in the perpendicular direction and small positive internal field in the longitudinal direction) and has nearly the same magnitude. These observations strongly support the assignment of a formal spin of $S = {}^3/_2$ at the iron sites in **1** and **2**.

EPR Spectrum. Figure 8 shows the X-band EPR spectrum of a mixture of **1** and **2** in the solid state at 5.3 K. The spectrum exhibits a broad resonance at $g \sim 5$ and a sharper peak at $g \sim 2$. There is no feature in the spectrum that is typical of $[Cu^{II}(MNT)]^{2-}$.[29,45] Typical $S = {}^5/_2$ Fe^{III} porphyrins exhibit an axial spectrum with $g_\perp \sim 6$ and $g_\parallel \sim 2$. Simple theory for an $S = {}^3/_2$ ground state would predict $g_\perp \sim 4$. Although the EPR spectrum is unusual, it indicates that the iron in **1** and **2** is $S = {}^3/_2$ with some $S = {}^5/_2$ character. Quantization of the signal by double integration (vs $[Fe(TPP)(OSO_2CF_3)]$ standard) indicates that ~5% of the total spin in the sample is observed.

Unlike the case for previously reported trinuclear $Fe^{III}/Cu^{II}/Fe^{III}$ complexes,[5] the observed EPR signal for this mixture is consistent from sample to sample and therefore may be the intrinsic signal of the mixture of **1** and **2** and not that of an impurity. The EPR spectrum does not appear to be that of an excited state of **1** and **2**, as the intensity of the signal does not change with temperature over the range 5.3–17.2 K.

Conclusion

The complexes **1**–**3** are structural variations of the same species—a neutral trinuclear $Fe^{III}/Cu^{II}/Fe^{III}$ unit with a weakly associated $[Cu^{III}(MNT)_2]^-$ anion, which probably dissociates as these compounds dissolve in noncoordinating solvents. Given the structural similarities among **1**–**3**, a predominantly $S = {}^3/_2$ spin state for both iron atoms in **3** is likely.

The magnetic susceptibility and Mössbauer measurements for the mixture of **1** and **2** support the $S = {}^3/_2$ spin-state assignment for the Fe^{III} atoms inferred from the structural results. The antiferromagnetic coupling ($J_{Fe-Cu} \approx -2$ cm^{-1}) between the metal centers in these complexes is not large enough to produce EPR silence. Therefore, the weakness of the EPR signal (~5% of the total iron) is more likely due to a second mechanism—relaxation broadening mediated by a small degree of exchange coupling through the bridging sulfur atoms.

These complexes serve as intriguing models for the active site of cytochrome *c* oxidase. They show that a bridging sulfur atom reproduces many structural features suggested by EXAFS studies and that such a bridge can mediate the interaction between the metals to produce an apparently diminished EPR signal (if not EPR silence).

Acknowledgment. C.M.E. and O.P.A. thank the National Institutes of Health (Grant No. GM-30306) for support of this work. The Nicolet R3m/E diffractometer and computing system was purchased with funds provided by the National Science Foundation (Grant No. CHE 8103011). B.R.S. thanks the Procter & Gamble Co. for support. W.E.H. thanks the National Science Foundation (Grant No. CHE 8807498) for support. We gratefully acknowledge Dr. Richard B. Frankel's assistance with the collection of the Mössbauer spectra while K.S. was on sabbatical leave at the National Magnet Lab, MIT. We also wish to thank Prof. G. R. Eaton (University of Denver) and Prof. S. S. Eaton (University of Colorado, Denver) for assistance in obtaining the EPR spectra.

Supplementary Material Available: Tables of crystallographic data, anisotropic thermal parameters, and calculated hydrogen atom positions (9 pages); listings of observed and calculated structure factors (81 pages). Ordering information is given on any current masthead page.

(42) Spartalian, K.; Lang, G.; Reed, C. A. *J. Chem. Phys.* **1979**, *71*, 1832.
(43) Dolphin, D. H.; Sams, J. R.; Tsin, T. B. *Inorg. Chem.* **1977**, *16*, 711.
(44) Epstein, L. M.; Straub, D. K.; Maricondi, C. *Inorg. Chem.* **1967**, *6*, 1720.
(45) Snaathorst, D.; Doesburg, H. M.; Perenboom, J. A. A.; Keijzers, C. P. *Inorg. Chem.* **1981**, *20*, 2526.